

Raman coupler for a trapped two-component quantum-degenerate Fermi gas

Sierk Pötting^{1,2,3}, Marcus Cramer^{1,4}, Weiping Zhang¹, and Pierre Meystre¹

¹*Optical Sciences Center, The University of Arizona, Tucson, AZ 85721*

²*Max-Planck-Institut für Quantenoptik, 85748 Garching, Germany*

³*Sektion Physik, Universität München, 80333 München, Germany*

⁴*Fachbereich Physik der Philipps-Universität, 35032 Marburg, Germany*

(Dated: November 18, 2018)

We investigate theoretically the Raman coupling between two internal states of a trapped low-density quantum-degenerate Fermi gas. In general, the trap frequencies associated with the two internal states can be different, leading to the onset of collapses and revivals in the population difference ΔN of the two internal states. This behavior can be changed drastically by two-body collisions. In particular, we show that under appropriate conditions they can suppress the dephasing leading to the collapse of ΔN , and restore almost full Rabi oscillations between the two internal states. These results are compared and contrasted to those for a quantum-degenerate bosonic gas.

PACS numbers: 03.75.Fi, 75.45.+j, 75.60.Ej

I. INTRODUCTION

Quantum-degenerate samples of low-density fermionic atomic gases [1, 2] are arguably even more interesting than their bosonic counterparts [3], due to the fundamental role played by the Pauli exclusion principle in their dynamics. This principle renders their experimental realization particularly difficult, since in the simplest case, the collisions that are essential in evaporative cooling largely disappear as the temperature of the sample goes to zero. For this reason, more elaborate techniques, involving e.g. the use of several isotopes, or sympathetic cooling via a bosonic system, have been used to achieve degeneracy [1]. Collisions also leave behind holes in the Fermi sea [4]; these holes are difficult to fill and are believed to limit the temperatures that can be achieved to about $0.2 T_F$, where T_F is the Fermi temperature.

From a theoretical viewpoint, Fermi systems also present a number of difficult challenges. In particular, they are not amenable to a mean-field description. Hence they cannot be analyzed in a classical-like formalism such as the Gross-Pitaevskii equation, which has proven remarkably powerful in describing many aspects of quantum-degenerate bosonic systems. On the other hand, the additional complexity of Fermi systems also offers much promise. One can hope to be able to manipulate them into strongly non-classical states, with potential applications in atom interferometry. Also, the nonlinear mixing of fermionic matter waves is expected to be very different from the bosonic case. As such, Fermi systems promise the extension of nonlinear atom optics [5] to a regime without counterpart in traditional nonlinear optics.

Just as is the case for bosons, a cornerstone of the manipulation of fermionic matter waves is their interaction with light. In this paper, we discuss the specific situation where transitions between two internal states of a trapped quantum-degenerate Fermi system at zero temperature are induced by Raman coupling. A straightforward generalization of this model could be used to de-

scribe an output coupler for an atom laser [6]. Our goal is two-fold: first, to understand the difference between the bosonic and fermionic dynamics; and second, to determine the role of two-body collisions on the evolution of the system.

We first consider the dynamics of the system in the absence of collisions. Section II introduces our model and derives the Heisenberg equations of motion for the relevant atomic fields, and section III compares the resulting dynamics with those for a corresponding Bose gas. Collisions are introduced in section IV. The resulting equations of motion are solved numerically in the framework of a time-dependent Hartree-Fock theory for the case of fermions, and in a standard mean-field theory for a bosonic sample. Again, we give a detailed comparison of the two situations, and illustrate how collisions can change the fermionic dynamics in a non-trivial fashion. Finally, Section V is a summary and conclusion.

II. MODEL

We consider a two-component quantum-degenerate atomic system trapped in a one-dimensional, harmonic potential with each component corresponding, e.g., to one internal hyperfine spin state. In general, the coupling of the atoms to the trapping field is different for the two (spin) components $|+\rangle$ and $|-\rangle$, so that they see trapping potentials of different frequencies ω_+ and ω_- . The two internal states are coupled by a Raman-type interaction of frequency ν equal to the spin-flip transition frequency of the atoms in the ground state of the two trapping potentials. This model, which is summarized on the diagram of Fig. 1, is described by the second-quantized Hamiltonian

$$\begin{aligned} \hat{\mathcal{H}} = & \int dx \hat{\Psi}_+^\dagger(x) H_+ \hat{\Psi}_+(x) + \int dx \hat{\Psi}_-^\dagger(x) H_- \hat{\Psi}_-(x) \\ & + \hbar g \int dx \left[e^{-i\nu t} \hat{\Psi}_+^\dagger(x) \hat{\Psi}_-(x) + h.c. \right], \end{aligned} \quad (1)$$

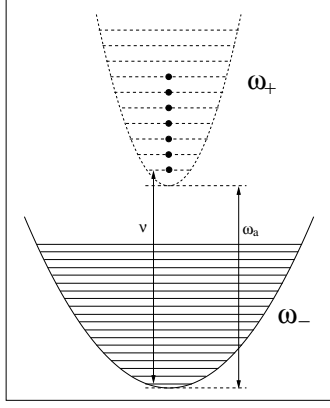


FIG. 1: Two-component Fermi gas in a harmonic trap. The trapping frequencies ω_+ and ω_- correspond to the two internal states, which are coupled via a spin-flip transition at frequency ν resonant with the frequency difference of the trap ground states.

where $\hbar g$ is the Raman coupling strength. The first-quantized Hamiltonian describing the trapping potentials associated with the internal states $|+\rangle$ and $|-\rangle$ is

$$H_{\pm} = -\frac{\hbar^2}{2m} \frac{\partial^2}{\partial x^2} + \frac{1}{2}m\omega_{\pm}^2 x^2 + E_{\pm}, \quad (2)$$

with E_{\pm} being the energy of the internal state $|\pm\rangle$. The Raman resonance condition is therefore, with $\omega_a = E_+ - E_-$,

$$\nu = \omega_a + (\omega_+ - \omega_-)/2. \quad (3)$$

We remark that this resonance condition effects only the coupling between the two trap ground states: the coupling between all other levels is off-resonant for $\omega_+ \neq \omega_-$. Hence, introducing a small detuning even for the ground states does not significantly alter the dynamics of the system.

The atomic field operators corresponding to the two traps obey the fermionic, respectively bosonic (anti)commutation relations

$$\begin{aligned} [\hat{\Psi}_i(x), \hat{\Psi}_j^\dagger(x')]_{\pm} &= \delta_{ij} \delta(x - x'), \\ [\hat{\Psi}_i(x), \hat{\Psi}_j(x')]_{\pm} &= 0, \\ [\hat{\Psi}_i^\dagger(x), \hat{\Psi}_j^\dagger(x')]_{\pm} &= 0, \end{aligned} \quad (4)$$

where $i, j = \{+, -\}$.

For the harmonic potentials at hand, the Heisenberg equations of motion for the atomic field operators take the same form, independently of whether the atoms are bosonic or fermionic. It is convenient to expand them in terms of eigenstates $\{u_n(x)\}$ of one of the trap Hamiltonians H_{\pm} , say, H_+ for concreteness, as

$$\hat{\Psi}_+(x, t) = \sum_n u_n(x) \hat{a}_n(t),$$

$$\hat{\Psi}_-(x, t) = \sum_n u_n(x) \hat{b}_n(t), \quad (5)$$

where the \hat{a}_n 's and \hat{b}_n 's satisfy either fermionic or bosonic commutation relations. In both cases, this expansion readily yields the Heisenberg equations of motion

$$\begin{aligned} i \frac{d\hat{a}_n}{d\tau} &= A_n \hat{a}_n + \tilde{g} \hat{b}_n, \\ i \frac{d\hat{b}_n}{d\tau} &= B_n \hat{b}_n + C_n \hat{b}_{n+2} + D_n \hat{b}_{n-2} + \tilde{g} \hat{a}_n, \end{aligned} \quad (6)$$

where we have introduced the coefficients

$$\begin{aligned} A_n &= \frac{1}{2}(\beta - 1) + n, \\ B_n &= \frac{1}{4}(\beta^2 - 1)(2n + 1) + n, \\ C_n &= \frac{1}{4}(\beta^2 - 1) \sqrt{(n + 2)(n + 1)}, \\ D_n &= \frac{1}{4}(\beta^2 - 1) \sqrt{n(n - 1)}, \end{aligned} \quad (7)$$

and the ratio

$$\beta = \omega_+/\omega_- \quad (8)$$

of the trap frequencies. The dimensionless time τ is scaled to ω_+ , $\tau = \omega_+ t$, and so is the dimensionless coupling strength $\tilde{g} = g/\omega_+$.

We emphasize that while the operator \hat{a}_n describes the annihilation of atoms in level n of the upper trap, a similar interpretation of the \hat{b}_n 's is not possible, since they result from the expansion of the field operator of atoms in the internal state $|-\rangle$ on the basis of the “+”-trap. Denoting the eigenstates of the single-atom Hamiltonian of the lower trap as $\{v_n(x)\}$, the “true” annihilation operators \hat{c}_n associated with the trapped atoms in the $|-\rangle$ internal state are related to the \hat{b}_n 's by the mapping

$$\hat{c}_n(t) = \sum_n T_{nm} \hat{b}_m(t), \quad (9)$$

where the mapping matrix element T_{nm} is the overlap integral

$$T_{nm} = \int dx v_n(x) u_m(x). \quad (10)$$

III. DYNAMICS

In this section, we compare the dynamics of ideal non-interacting bosonic and fermionic systems evolving under the influence of the Raman coupling. We proceed by numerically solving the Heisenberg equations of motion (6) for a sample of N atoms initially in the internal state $|+\rangle$ and at temperature $T = 0$. For bosonic atoms, all atoms are therefore initially in the “+”-trap ground state, while

for fermions they fill the lowest N trap levels. The corresponding initial states are correspondingly

$$|\psi_F(0)\rangle = \prod_{i=0}^{N-1} \hat{a}_i^\dagger |0\rangle_+ \otimes |0\rangle_-, \quad (11)$$

in the case of fermions, and

$$|\psi_B(0)\rangle = \frac{1}{\sqrt{N!}} \hat{a}_0^\dagger |0\rangle_+ \otimes |0\rangle_- \quad (12)$$

for bosonic atoms.

We consider, first, the case of noninteracting fermionic atoms. For trap frequencies approximately equal, $\beta \simeq 1$, Eq. (6) suggests the existence of two limiting situations, at least in the case of fermions. (We will revisit this point when discussing low-temperature bosonic systems.) In the first one, which we call the “strong-coupling regime” in the following, $\tilde{g} \approx N$, so that the inter-trap coupling dominates the dynamics and the intra-trap coupling terms $\hat{b}_{n\pm 2}$ can largely be ignored. In contrast, the “weak-coupling regime” $\tilde{g} \ll N$ is dominated by intra-trap coupling.

As a first measure of the system dynamics, Fig. 2 shows the difference

$$\begin{aligned} \Delta N(\tau) &= \frac{1}{N} \int dx \left[\langle \hat{\Psi}_+^\dagger(x) \hat{\Psi}_+(x) \rangle - \langle \hat{\Psi}_-^\dagger(x) \hat{\Psi}_-(x) \rangle \right] \\ &= \frac{1}{N} \sum_n \left(\langle \hat{a}_n^\dagger(\tau) \hat{a}_n(\tau) \rangle - \langle \hat{c}_n^\dagger(\tau) \hat{c}_n(\tau) \rangle \right). \end{aligned} \quad (13)$$

between the populations of the “+” and “-” traps. Fig. 2a is for the strong-coupling regime, and Fig. 2b for the weak-coupling regime.

One can gain some intuitive understanding of the strong-coupling regime by remarking that in that regime, intra-trap transitions remain small, so that the Raman coupling is predominantly between levels of the two traps with equal quantum number n . To lowest order, these transitions are all at the Rabi frequency \tilde{g} . However, this simplest description cannot explain the result of Fig. 2a. Rather, it is necessary to include at least their lowest-order corrections, i.e.,

$$\Omega_n = \sqrt{\tilde{g}^2 + \frac{1}{4} (A_n - B_n)^2} \simeq \tilde{g} + \left(\frac{(\beta - 1)^2}{8\tilde{g}} \right) n^2. \quad (14)$$

Such an n -dependence of Rabi frequencies is known to lead to collapse and revival phenomena, as was first discussed in the context of the Jaynes-Cummings model [7], where $\Omega_n \propto \sqrt{n}$. This is precisely the type of behavior exhibited by ΔN in the strong-coupling regime. Because of the n^2 -dependence of Ω_n , it is expected that the lowest trap levels, i.e. the atoms in the deep Fermi sea, play a dominant role in the appearance of the revivals. We verified that the populations of the lowest trap levels indeed oscillate more or less in phase, while those of higher n levels dephase rapidly.

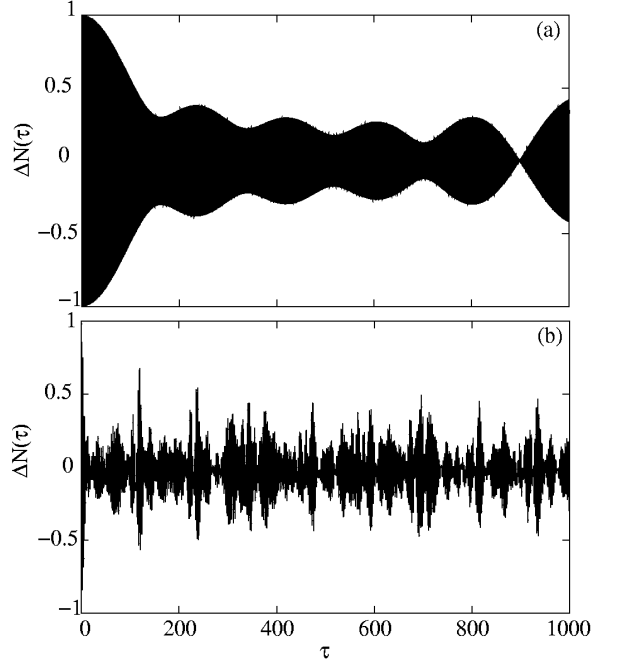


FIG. 2: $\Delta N(\tau)$ for $N = 10$ fermions and trap ratio $\beta = 0.9$, as obtained from a numerical integration of Eqs. (6): (a) strong coupling regime with $\tilde{g} = 10.0$; (b) weak coupling regime with $\tilde{g} = 1.0$. The dimensionless time τ is in units of $1/\omega_+$.

We remark that both collapses and revivals of ΔN disappear when the two trap frequencies are identical, since for $\beta = 1$, we have $A_n = B_n = n$ and hence $\Omega_n = \tilde{g}$. In addition, intra-trap transitions vanish in that case, due to $C_n = D_n = 0$.

Fig. 2b shows the inversion ΔN between the total trap populations in the weak-coupling regime, $\tilde{g} \ll N$. In this limit, inter-trap and intra-trap coupling occur on similar timescales. Immediately following a Raman transition from the $|+\rangle$ to the $|-\rangle$ internal state, the population of the “-”-trap starts to undergo a redistribution between its levels. The combined effects of the intra- and inter-trap transitions result in that case in a random-looking evolution of $\Delta N(t)$ of Fig. 2b.

We now briefly turn to the case of a Bose gas. For a sample at zero-temperature, $T = 0$, and initially in the internal state $|+\rangle$, all atoms are in the ground state of the “+”-trap at $\tau = 0$. As a result, the strong-coupling regime is characterized by almost perfect Rabi oscillations of the atomic population between the two trap ground states, with a very small fraction of the atoms coupling to higher modes due to intra-trap transitions. This behavior is also largely preserved for $\beta^2 - 1 \ll \tilde{g} \ll N$. (We recall that for fermions the right-hand side of this inequality corresponds to the weak-coupling regime, dominated by intra-trap transitions.) This difference between bosons and fermions can readily be understood from Eqs. (6), which show that in the $T = 0$ bosonic

case, intra-trap coupling first occurs between the levels $n = 0$ and $n = 2$ of the “-”-trap, with coupling coefficient $D_2 = (\beta^2 - 1)/4$. As long as this coupling remains small compared to the inter-trap coupling \tilde{g} , the system acts effectively as a two-mode system. In other words, for low temperature bosonic systems, the weak-coupling regime is not characterized by $\tilde{g} \approx N$ as is the case for fermions, but rather by $\tilde{g} \ll \beta^2 - 1$.

As is to be expected, the difference between fermionic and bosonic systems is reduced as T is increased. At first, the sharp edge of the Fermi-Dirac distribution softens, resulting in slightly reduced (strong-coupling) collapses and revivals of the fermionic system. On the other hand, for $T \neq 0$, bosons occupy higher trap states, resulting in a spread in Rabi frequencies participating in the population difference signal. This in turn leads to collapses and revivals rather than the perfect $T = 0$ Rabi oscillations. Increasing the temperature further leads of course to undistinguishable behaviors of the bosonic and fermionic systems.

IV. COLLISIONS

In this section, we discuss the effect of collisions on the preceding results. Collisions are of course central to the dynamics of quantum-degenerate atomic systems. They are essential in the evaporative cooling of the sample, and also provide a nonlinearity that can lead to the nonlinear mixing of matter waves. In bosonic systems, much new physics can be studied, e.g. by changing the sign of the scattering length of s -wave collisions. In the case of fermions the creation of holes in the Fermi sea, and the filling of these holes by additional collisions results in a heating that appears to fundamentally limit the temperatures at which these samples can be cooled [4]. First, we discuss the way collisions impact the operation of the Raman coupler in the case of fermions, and later compare these results with those for a bosonic sample.

It is well known that in fermionic atoms, the Pauli exclusion principle forbids the existence of s -wave scattering between atoms in the same internal state. In addition, p -wave scattering is generally negligible. Hence two-body collisions are described by the Hamiltonian

$$\hat{\mathcal{H}}_{\text{col}} = U_0 \int dx \hat{\Psi}_+^\dagger(x) \hat{\Psi}_-^\dagger(x) \hat{\Psi}_-(x) \hat{\Psi}_+(x), \quad (15)$$

where $U_0 = 4\pi\hbar^2 a\rho/m$ is the interaction strength with a being the s -wave scattering length and ρ the characteristic density of the system. Again, we expand the field operators according to Eq. (5) in terms of the basis $\{u_n\}$ and obtain

$$\hat{\mathcal{H}}_{\text{col}} = U_0 \sum_{i,j,k,l} U_{ijkl} \hat{a}_i^\dagger \hat{b}_j^\dagger \hat{b}_k \hat{a}_l, \quad (16)$$

where the matrix element

$$U_{ijkl} = \int dx u_i(x) u_j(x) u_k(x) u_l(x) \quad (17)$$

characterizes the scattering between different levels. We note that U_{ijkl} is symmetric under permutations.

In the presence of this quartic Hamiltonian, the Heisenberg equations of motion for the operators a_n and b_n involve cubic combinations of operators. To close this system of equations, we invoke a time-dependent Hartree-Fock ansatz, which has proved to be very successful in the treatment of many-particle quantum systems [8], to factorize products of operators, of the generic form $\hat{b}_i^\dagger(\tau) \hat{b}_j(\tau) \hat{a}_k(\tau)$, by

$$\hat{b}_i^\dagger(\tau) \hat{b}_j(\tau) \hat{a}_k(\tau) \approx \langle \hat{b}_i^\dagger(\tau) \hat{b}_j(\tau) \rangle \hat{a}_k(\tau) - \langle \hat{b}_i^\dagger(\tau) \hat{a}_k(\tau) \rangle \hat{b}_j(\tau), \quad (18)$$

where the expectation value is over the state $|\psi_F(0)\rangle$ since we work in the Heisenberg picture. At this level of approximation, we neglect all contributions from pairing. This factorization scheme readily yields the time-dependent Hartree-Fock equations of motion (in dimensionless variables)

$$\begin{aligned} i \frac{\partial \hat{a}_n}{\partial \tau} &= \sum_k \left[(A_n \delta_{nk} + Q_{nk}^{bb}) \hat{a}_k - \left(Q_{nk}^{ab*} - \tilde{g} \delta_{nk} \right) \hat{b}_k \right] \\ i \frac{\partial \hat{b}_n}{\partial \tau} &= \sum_k \left[(B_n \delta_{nk} + Q_{nk}^{aa}) \hat{b}_k - \left(Q_{nk}^{ab} - \tilde{g} \delta_{nk} \right) \hat{a}_k \right] \\ &+ C_n \hat{b}_{n+2} + D_n \hat{b}_{n-2}, \end{aligned} \quad (19)$$

where we have introduced the time-dependent coefficients

$$\begin{aligned} Q_{nk}^{aa}(\tau) &= \tilde{U}_0 \sum_{i,j} U_{nijk} \langle \hat{a}_i^\dagger(\tau) \hat{a}_j(\tau) \rangle \\ Q_{nk}^{bb}(\tau) &= \tilde{U}_0 \sum_{i,j} U_{nijk} \langle \hat{b}_i^\dagger(\tau) \hat{b}_j(\tau) \rangle \\ Q_{nk}^{ab}(\tau) &= \tilde{U}_0 \sum_{i,j} U_{nijk} \langle \hat{a}_i^\dagger(\tau) \hat{b}_j(\tau) \rangle, \end{aligned} \quad (20)$$

and $\tilde{U}_0 = U_0/\hbar\omega_+$ is a dimensionless interaction strength.

The effect of collisions is illustrated in Figs. 3a,b, which show the population inversion $\Delta N(\tau)$ for two values of the interaction strength \tilde{U}_0 .

For weak enough collisions, the dynamics of the system is not significantly altered, as should of course be expected. However, we observe a quantitative change in the dynamics of ΔN as \tilde{U}_0 is increased. Instead of a collapse and revivals, $\Delta N(\tau)$ now undergoes nearly full Rabi oscillations.

A first hint at the cause of this changed behavior is offered by Fig. 4, which shows a snapshot of the level populations in the “+”-trap for the cases of Fig. 3a and 3b, respectively. We observe that the smaller value of \tilde{U}_0 corresponds to an inhomogeneous level population distribution, whereas the higher nonlinearity causes the trap levels to be almost equally populated.

A more quantitative understanding of the role of collisions can be gained by estimating how the nonlinear terms in Eq. (19) modify the (collisionless) Rabi frequency. A numerical evaluation of the coefficients U_{ijkl}

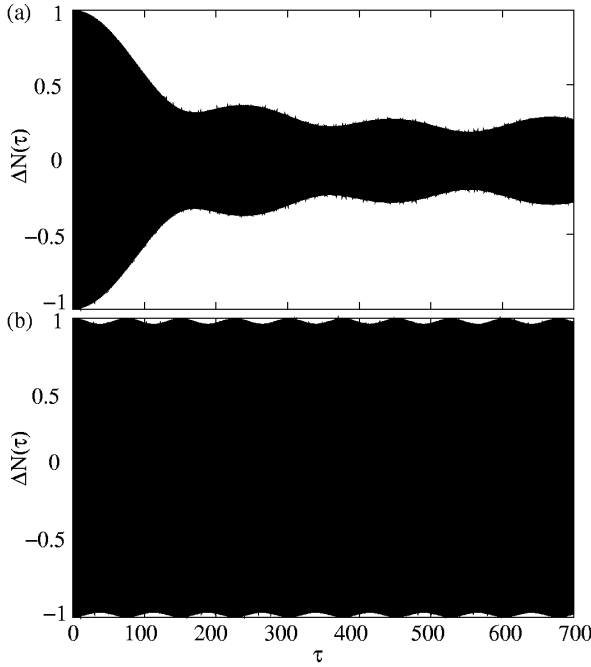


FIG. 3: Population difference $\Delta N(\tau)$ for $N = 10$ fermions, a trap ratio $\beta = 0.9$ and in the strong-coupling regime $\tilde{g} = 10.0$. The plots, which result from the numerical integration of Eqs. (19), are for different strengths of the two-body collisions: (a) $\tilde{U}_0 = 0.01$; (b) $\tilde{U}_0 = 0.1$. Dimensionless time τ in units of $1/\omega_+$.

shows that elastic collisions, $i = j = k = l$, dominate the dynamics of the system. In addition, U_{nnnn} turns out to be a decreasing function of n . Keeping the elastic contributions to the collision-induced dynamics only, and neglecting as in the strong-coupling regime of section III the effects of intra-trap coupling terms $\hat{b}_{n\pm 2}$, one finds that as a result of collisions Eq. (14) is approximately changed to

$$\Omega_n^{NL}(\tau) = \sqrt{g^2 + \frac{1}{4} (A_n - B_n + Q_{nn}^{bb}(\tau) - Q_{nn}^{aa}(\tau))^2}. \quad (21)$$

Fig. 5 shows, as a function of \tilde{U}_0 , the time-dependent Rabi frequencies $\Omega_n^{NL}(\tau)$ averaged over a time interval Θ large compared to their inverse,

$$\bar{\Omega}_n = \frac{1}{\Theta} \int_0^\Theta d\tau \Omega_n^{NL}(\tau). \quad (22)$$

Because U_{nnnn} is a decreasing function of n , its contribution tends to compensate the n^2 dependence of Eq. (14). As a result, there is a range of collision strengths for which the dependence of $\Omega_n^{NL}(\tau)$ on n largely disappears. In this range, paradoxically, the dynamics of the collision-dominated Fermi system resembles that of a collisionless Bose system. From this admittedly crude argument – which is however consistent with our full nu-

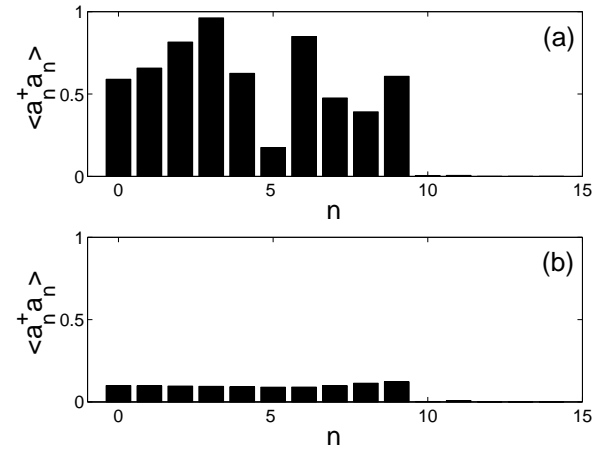


FIG. 4: Occupation of the first 15 upper trap levels at the dimensionless time $\tau = 490/\omega_+$, (a) for the parameters of Fig. 3a; and (b) for the parameters of Fig. 3b.

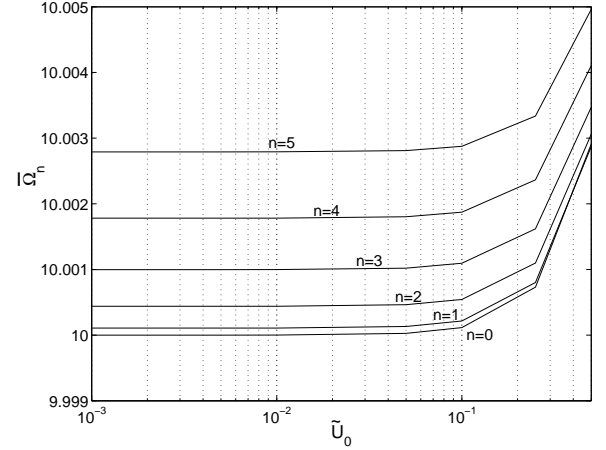


FIG. 5: Semi-logarithmic plot of the time-averaged generalized Rabi frequencies for the six lowest trap levels as a function of the nonlinear parameter, otherwise the same parameters as in Fig. 3 are used. $\bar{\Omega}_n$ is given in units ω_+ , \tilde{U}_0 in units of $\hbar\omega_+$.

merical results – we also conjecture that for even larger \tilde{U}_0 , the approximate cancellation of the n -dependence of the Rabi frequencies will disappear and we expect an overall dephasing and decay of the population difference $\Delta N(t)$. It has unfortunately proven prohibitive to try and check this conjecture numerically.

We now turn to the case of bosonic atoms. Bose statistics allows for s -wave collisions between atoms in the same spin state, so that the collisional Hamiltonian is now

$$\hat{H}_{\text{col}} = U_+ \int dx \hat{\Psi}_+^\dagger(x) \hat{\Psi}_+^\dagger(x) \hat{\Psi}_+(x) \hat{\Psi}_+(x)$$

$$\begin{aligned}
& + U_- \int dx \hat{\Psi}_-^\dagger(x) \hat{\Psi}_-^\dagger(x) \hat{\Psi}_-(x) \hat{\Psi}_-(x) \\
& + 2U_x \int dx \hat{\Psi}_+^\dagger(x) \hat{\Psi}_-^\dagger(x) \hat{\Psi}_+(x) \hat{\Psi}_-(x), \quad (23)
\end{aligned}$$

where the U_i , $i = \{+, -, x\}$ characterize the strength of the collisions. In the following we assume for simplicity $U_+ = U_- = U_0$ and $U_x = \eta_x U_0$.

To truncate the Heisenberg equations of motion for the field operators, we now invoke a mean-field approximation, factorize all products of operators, and replace the resulting expectation values by time-dependent c -numbers. This gives

$$\begin{aligned}
i \frac{d\langle \hat{a}_n \rangle}{d\tau} &= \sum_k (A_n \delta_{nk} + Q_{nk}^{aa} + \eta_x Q_{nk}^{bb}) \langle \hat{a}_k \rangle + \tilde{g} \langle \hat{b}_n \rangle \\
i \frac{\partial \langle \hat{b}_n \rangle}{\partial \tau} &= \sum_k (B_n \delta_{nk} + Q_{nk}^{bb} + \eta_x Q_{nk}^{aa}) \langle \hat{b}_k \rangle + \tilde{g} \langle \hat{a}_n \rangle \\
& + C_n \langle \hat{b}_{n+2} \rangle + D_n \langle \hat{b}_{n-2} \rangle, \quad (24)
\end{aligned}$$

where

$$\begin{aligned}
Q_{nk}^{aa}(\tau) &= 2\tilde{U}_0 \sum_{i,j} U_{n,i,j,k} \langle \hat{a}_i(\tau) \rangle^* \langle \hat{a}_j(\tau) \rangle \\
Q_{nk}^{bb}(\tau) &= 2\tilde{U}_0 \sum_{i,j} U_{nijk} \langle \hat{b}_i(\tau) \rangle^* \langle \hat{b}_j(\tau) \rangle, \quad (25)
\end{aligned}$$

and the expectation values are with respect to the state $|\psi_B(0)\rangle$. Figure 6 shows the inversion $\Delta N(\tau)$ for a sample of bosonic atoms initially in the internal state $|+\rangle$ for a nonlinear parameter $\tilde{U}_0 = 0.5$. In contrast to the case where collisions are absent and we have full Rabi oscillations, c.f. Sec. III, here one starts observing a damping of the oscillations. This is clearly a result of the scattering of atoms into higher trap states. This is illustrated in Fig. 7, which shows the population of the first upper trap levels at a fixed time. The transitions between the populated trapped states are characterized by n -dependent Rabi-frequencies, leading to the onset of a dephasing process resembling the situation for noninteracting fermions [9]. We see, then, that in the case of interacting bosons, intra-trap scattering is an important element of the dynamics of the Raman coupler, which rapidly evolves to a multimode behavior; in contrast in the intrinsically multimode fermionic case U_{ijkl} tends to reduce the spread in Rabi frequencies and thus inhibits dephasing.

A remarkable property of the bosonic trap population distribution is that only even trap levels are occupied, see Fig. 7. This is a combined result of three facts: (a) at $T = 0$ all atoms are initially in the ground state of one of the traps; (b) s -wave scattering only couples trap states of same parity, as expressed by the symmetry properties of the collision matrix from Eq. 17; (c) intra-trap coupling only couples trap levels with $\Delta n = 2$, see Eq. (6).

It is known from nonlinear optics [10] and atom optics [11] that systems governed by a pair of coupled nonlinear

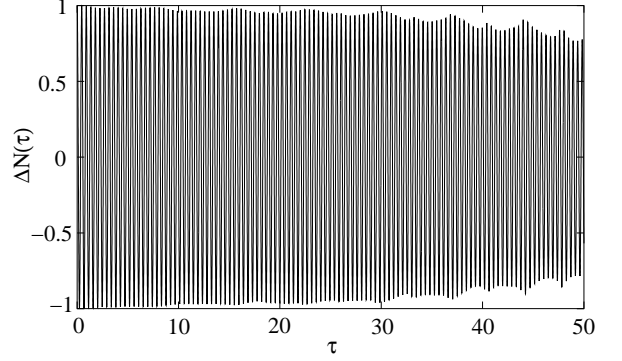


FIG. 6: $\Delta N(\tau)$ for $N = 20$ bosons, trap ratio $\beta = 0.9$, linear coupling $\tilde{g} = 7.0$ and $\eta_x = 1.5$, from the numerical solution of Eq. (24) with $\tilde{U}_0 = 0.5$. Dimensionless time τ in units of $1/\omega_+$

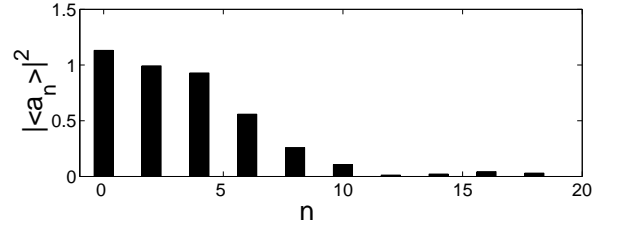


FIG. 7: Level population of the “+”-trap at the dimensional time $\tau = 25/\omega_+$ for the parameters of Fig. 6.

Schrödinger equations can reach a regime where the nonlinear phase shifts dominate their dynamics. Such two-mode systems exhibit Rabi oscillations for small nonlinearities, but mode-coupling is inhibited above a certain strength of the nonlinearity. This effect is absent in the present multimode system, a result of the strong intermode scattering.

V. SUMMARY

The Raman coupling between two internal states of a trapped Fermi gas exhibits a rich dynamics, quite different from its bosonic counterpart. This is of course due primarily to the fact that a Fermi gas occupies a large number of trap states, and hence can never be approximated as a two-mode system. In particular, we have identified two limiting regimes, dependent upon whether inter-trap or intra-trap dynamics is dominant. In the general situation where the traps associated with the two internal states have different frequencies, the first of these regimes leads to dynamics characterized by collapses and revivals. However, two-body collisions can under appropriate conditions inhibit this behavior, making the collision-dominated Fermi system more similar to

a collisionless Bose system.

The numerical analysis of fermionic systems appears to be presently limited to very small numbers N of atoms, a result of the large memory requirements associated with the need to keep track of a large number of quantum states. Indeed, most of our numerical results are limited to N on the order of 10 (especially for the collisional calculations), and even this required rather large computing facilities. Despite this limitation and its associated lack of quantitative predictions, our analysis sheds useful light on the dynamics of trapped Fermi systems, in particular in the presence of collisions, and will provide useful guidance in understanding more realistic trapped Fermi gases in three dimensions and with a large number of fermionic

atoms.

Acknowledgments

We thank J. V. Moloney for providing us with CPU time on his parallel cluster, and E. M. Wright and C. P. Search for valuable discussions. This work is supported in part by the US Office of Naval Research under Contract No. 14-91-J1205, by the National Science Foundation under Grant No. PHY-0098129, by the US Army Research Office, by NASA, and by the Joint Services Optics Program.

- [1] B. DeMarco and D. S. Jin, *Science* **285**, 1703 (1999); A. G. Truscott *et al.*, *Science* **291**, 2570 (2001); B. DeMarco *et al.*, *Phys. Rev. Lett.* **86**, 5409 (2001); F. Schreck *et al.*, *Phys. Rev. Lett.* **87**, 080403 (2001).
- [2] H. T. C. Stoof *et al.*, *Phys. Rev. Lett.* **76**, 10 (1996); M. Houbiers *et al.*, *Phys. Rev. A* **56**, 4864 (1997); G. Bruun *et al.*, *Eur. Phys. J. D* **7**, 433 (1999); L. You and M. Marinescu, *Phys. Rev. A* **60**, 2324 (1999); M. A. Baranov, *JETP Lett.* **64**, 301 (1996); E. Timmermans *et al.*, *Phys. Lett. A* **285**, 228 (2001); E. Holland *et al.*, *Phys. Rev. Lett.* **87**, 120406 (2001).
- [3] M. H. Anderson *et al.*, *Science* **269**, 198 (1995); K. B. Davis *et al.*, *Phys. Rev. Lett.* **75**, 3969 (1995); C. C. Bradley *et al.*, *Phys. Rev. Lett.* **75**, 1687 (1995).
- [4] E. Timmermans, *Phys. Rev. Lett.* **87**, 240403 (2001).
- [5] P. Meystre, *Atom Optics* (Springer-Verlag, New York, 2001).
- [6] M. O. Mewes, M. R. Andrews, D. M. Kurn, D. S. Durfee, C. G. Townsend, and W. Ketterle, *Phys. Rev. Lett.* **78**, 582 (1997); E. W. Hagley, L. Deng, M. Kozuma, J. Wen, K. Helmerson, S. L. Rolston, W. D. Phillips, *Science* **283**, 1706 (1999); I. Bloch, T. W. Hänsch, and T. Esslinger, *Phys. Rev. Lett.* **82**, 3008 (1999).
- [7] F. W. Cummings, *Phys. Rev.* **140**, A1051 (1965).
- [8] A. L. Fetter and J. D. Walecka, *Quantum theory of many-particle systems* (McGraw-Hill, San Francisco, 1971).
- [9] The choice of a given number of modes in the numerical simulations limits the evolution time to values such that the population of modes close to the numerical cut-off point remains small.
- [10] S. M. Jensen, *IEEE Journal of Quantum Electronics* **QE-18**, 1580 (1982).
- [11] K. J. Schernthanner, G. Lenz, and P. Meystre, *Phys. Rev. A* **51**, 3121 (1995).